Bump-on-tail instability in space plasmas

Susmita Sarkar, Samit Paul, and Raicharan Denra

Bump-on-tail instability in space plasmas

Susmita Sarkar,[a)] Samit Paul,[b)] and Raicharan Denra[c)]
*Department of Applied Mathematics, University of Calcutta, 92, Acharya Prafulla Chandra Road,
Kolkata 700009, India*

Bump-on-tail instability of Langmuir waves propagating in unmagnetized Lorentzian plasma modeled by a Kappa velocity distribution with spectral index κ has been investigated in this paper. Growth rate of this microinstability has been determined analytically from the Langmuir wave dispersion relation. Change in the maximum growth rate with increasing κ has been numerically estimated for different number density and temperature ratios using solar wind data. © 2015 AIP Publishing LLC. [http://dx.doi.org/10.1063/1.4933041]

I. INTRODUCTION

Bump-on-tail instability in plasma is an important micro-instability where the electron velocity distribution function is multiple peaked. The additional population of particles moves relative to the back ground plasma producing a positive velocity gradient of the distribution function. The part AB in Figure 1 having positive velocity gradient shows that number of electrons with velocity higher than wave phase velocity v_{ph} is greater than number of electrons with velocity lower than wave phase velocity. Thus, the number of electrons that transfer energy to the Langmuir wave is greater than the number of electrons to which the wave transfers energy. In this situation, Langmuir waves become unstable and grow exponentially in magnitude. A limited number of particles are in resonance, which actually drives this instability. All other charge particles feel the wave electric field and participate in the oscillation. This "bump-on-tail" instability is an example of a class of micro-instabilities, which is a well-known phenomenon in Maxwellian plasma.[1,2]

The natural space environment, e.g., planetary magnetospheres, solar wind, and astrophysical plasmas, is generally observed to possess a particle distribution function with a non-Maxwellian tail and its presence being widely confirmed by spacecraft measurements.[3] Such deviations from the Maxwellian distributions are expected to exist in any low-density plasma in the universe, where binary collisions of charges are sufficiently rare. These are well described by the so-called Kappa (κ) or generalized Lorentzian velocity distributions functions.[4,5] The Kappa distribution is very convenient to model such velocity distribution functions, since it fits both the thermal and the suprathermal parts of the observed energy spectra.[5] These distributions have Maxwellian-like core with high energy tails decreasing as a power law in particle speed as shown in Fig. 2. The conventional isotropic, three dimensional form of the Kappa velocity distribution function for electrons in equilibrium may be written as[5]

$$f_{e0}(v_x,v_y,v_z)=n_e(\pi\theta^2\kappa)^{-3/2}\frac{\Gamma(\kappa+1)}{\Gamma(\kappa-1/2)}\left[1+\frac{v_x^2+v_y^2+v_z^2}{\kappa\theta^2}\right]^{-(\kappa+1)},$$

(1)

where $\theta=\left[\frac{(2\kappa-3)K_BT}{\kappa m_e}\right]^{1/2}$ is the thermal velocity, m_e, n_e, T are, respectively, the mass, number density, temperature, $\vec{v}=(v_x,v_y,v_z)$ is the velocity of electrons, $\Gamma(x)$ is the Gamma function, and K_B is the Boltzmann constant. The value of the index κ determines the slope of the energy spectrum of the suprathermal particles forming the tail of the velocity distribution functions. In the limit $\kappa\to\infty$, this Kappa distribution reduces to Maxwellian distribution. Kappa distributions with $2<\kappa<6$ have been found to fit the observations and satellite data in the solar wind, the terrestrial magnetosphere; the magnetosheath, the magnetosphere of other planets like Mercury, Jupiter, Saturn, and Uranus as observed by Ulysses, Cassini, and the Hubble Space Telescope.[6]

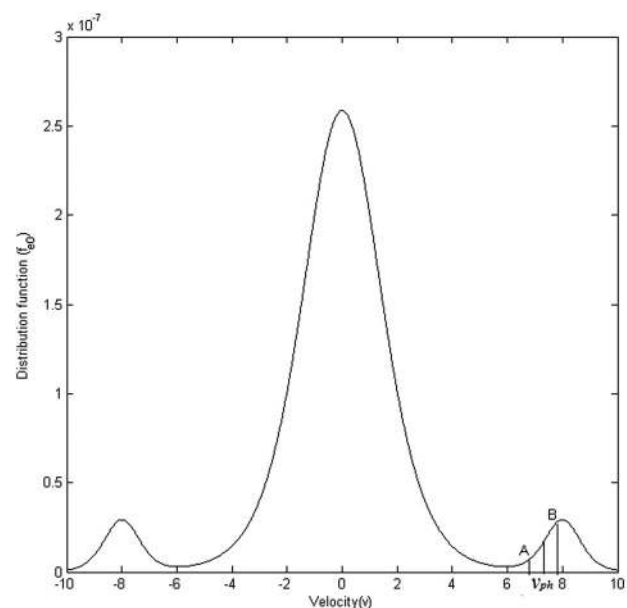Study of different instabilities in space plasma is an emerging area of plasma research since last century. A tool

FIG. 1. A multiple peaked electron velocity distribution function. AB indicates the positive slope of the bump.

a)Electronic mail: susmita62@yahoo.co.in
b)Electronic mail: samitpaul4@gmail.com
c)Electronic mail: raicharanroykolkata@gmail.com
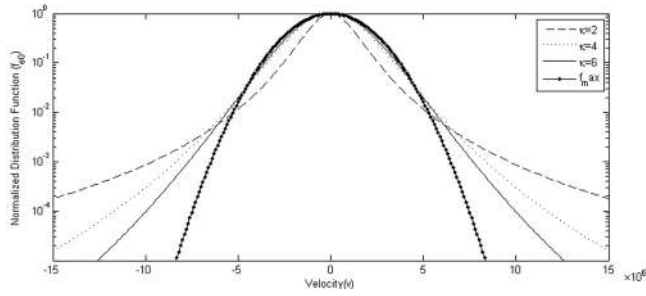
22, 102109-1

FIG. 2. A plot of normalized kappa distribution function for different kappa indices.

for analyzing microinstabilities in space plasmas was modeled by Summers and Thorne[7] with a generalized Lorentzian (kappa) distribution. This tool was used to study plasma microinstabilities driven by a generalized Lorentzian (kappa) loss-cone distribution for fully ionized, homogeneous, hot plasma in a uniform magnetic field.[8] The dielectric tensor, modified plasma dispersion function, and dispersion relation for whistler mode instability in an infinite magnetoplasma were obtained in the case of cold plasma injection to background hot anisotropic generalized bi-Lorentzian (κ) plasma in the presence of external perpendicular ac electric field.[9] The same whistler mode instability with parallel ac field in Lorentzian plasma was analytically studied by Pandey et al.[10] Ki and Jung[11] showed that nonthermal character of Lorentzian electrons in dusty plasmas decreases the growth rate of Bunemann instability caused by the interaction between streaming ions and stationary dust grains. Study on the effect of electron-ion collision on Weibel instability in a Kappa distributed unmagnetized plasma showed that growth rate of the instability is higher for the Maxwellian particles; however, in the presence of collisions, the suprathermal particles result in lower damping of Weibel mode.[12]

In this paper, we have studied the bump-on-tail instability of Langmuir waves in a collision-less, unmagnetized Lorentzian plasma, where electron velocity distribution has been modeled by a generalized Kappa distribution. This study shows that Langmuir waves propagating parallel to the particle velocity in the bump are unstable. Maximum growth rate of this instability decreases with increasing kappa values and approaches to the value attained in Maxwellian plasma.[2] Moreover, magnitude of the maximum growth of the wave is high when number density of electrons in bump is high and temperature of the electrons in the bump is low. Results have been applied to the solar wind.

In Section II of the paper, a general mathematical formalism of the instability has been presented. Based on this formalism, "bump-on-tail" instability in Lorentzian plasma has been developed in Section III. Numerical estimations with solar wind data have been presented in Section IV. Results have been concluded in Section V.

II. GENERAL MATHEMATICAL FORMALISM

For an isotropic plasma, information about the Langmuir wave characteristics is obtained from the dispersion function[2,13]

$$D(k,\omega) = 1 - \frac{\omega_{pe}^2}{k^2} \int \frac{\frac{\partial f_{e0}}{\partial v}}{v - \frac{\omega}{k}} dv, \qquad (2a)$$

where $\omega_{pe} \left(= \sqrt{\frac{4\pi e^2 n_e}{m_e}} \right)$ is the electron plasma frequency, m_e, n_e, f_{e0} are, respectively, mass, number density, and equilibrium velocity distribution of electrons, v is the electron velocity, ω and k are the frequency and wave number of the Langmuir wave.

The normal modes of oscillation of plasma are those wavelike disturbances that persist long after dying out the initial disturbance. Those normal modes are characterized by the zeros of $D(k,\omega) = 0$, for which the frequency ω is almost purely real, with small negative imaginary part. Assuming $\omega = \omega_r + i\omega_i$, where ω_r and ω_i are real and imaginary parts of the frequency ω, $D(k,\omega)$ can be expressed as

$$D(k,\omega) = D_r(k,\omega) + iD_i(k,\omega), \qquad (2b)$$

where $D_r(k,\omega)$ and $D_i(k,\omega)$ are real and imaginary parts of $D(k,\omega)$, respectively.

For weak damping $\omega_i \ll \omega_r$, $D(k,\omega)$ in (2a) can be expressed in the form[2]

$$D(k,\omega) = D_r(k,\omega_r) + i\omega_i \frac{\partial D_r(k,\omega)}{\partial \omega}\bigg|_{\omega=\omega_r} + iD_i(k,\omega). \quad (3)$$

The real frequency ω_r can be found by solving

$$D_r(k,\omega_r) = 1 - \frac{\omega_{pe}^2}{k^2} \int \frac{\frac{\partial f_{e0}}{\partial v}}{\left(v - \frac{\omega_r}{k} \right)} dv = 0 \qquad (4)$$

and the growth rate of the wave ω_i is found from

$$\omega_i = -\frac{D_i(k,\omega_r)}{\frac{\partial D_r(k,\omega_r)}{\partial \omega_r}}, \qquad (5)$$

$$\text{with } D_i = -\frac{\pi \omega_{pe}^2}{k^2} \left(\frac{\partial f_{e0}}{\partial v} \right)_{v=\frac{\omega_r}{k}}. \qquad (6)$$

The real part of the dielectric function $D_r(k,\omega_r)$ gives the response of the bulk of the plasma to the electric field in the plasma wave. The growth or damping rate ω_i gives the effect of the class of particles that are exactly in resonance with the wave.[2]

III. APPLICATION IN LORENTZIAN PLASMA

In space plasmas, such as planetary magnetosphere, the solar wind, and cometary tails, it has been observed that particle velocity distribution possesses a non Maxwellian high-energy tail. In practice, they are effectively modeled by Lorentzian distributions containing index kappa (κ). For studying "bump-on-tail" instability in Lorentzian plasma, we consider an additional population of high energy electrons with velocity v_0 streaming in the z direction. This has been modeled by the following multipeaked kappa electron velocity distribution

$$f_{e0}(v_x, v_y, v_z) = \frac{n_1}{n_e} \left(\pi\kappa\theta_1^2\right)^{-\frac{3}{2}} \frac{\Gamma(\kappa+1)}{\Gamma\left(\kappa-\frac{1}{2}\right)} \left[1 + \frac{v_x^2 + v_y^2 + v_z^2}{\kappa\theta_1^2}\right]^{-(\kappa+1)} + \frac{n_2}{n_e} \delta(v_x)\delta(v_y) \left(\pi\kappa\theta_2^2\right)^{-\frac{1}{2}} \frac{\Gamma(\kappa)}{\Gamma\left(\kappa-\frac{1}{2}\right)} \frac{1}{2}$$

$$\times \left[\left(1 + \frac{(v_z - v_0)^2}{\kappa\theta_2^2}\right)^{-\kappa} + \left(1 + \frac{(v_z + v_0)^2}{\kappa\theta_2^2}\right)^{-\kappa}\right], \tag{7}$$

where (n_1, n_2) and (T_1, T_2) are number densities and temperatures of electrons in the thermal region and the bump region, respectively, $\theta_1 \left(= \left[\frac{(2\kappa-3)K_B T_1}{\kappa m_e}\right]^{\frac{1}{2}}\right)$ and $\theta_2 \left(= \left[\frac{(2\kappa-3)K_B T_2}{\kappa m_e}\right]^{\frac{1}{2}}\right)$ are their respective thermal velocities. Population of suprathermal electrons streaming with velocity v_0 produces relative velocity $(v_z - v_0)$ in positive and $(v_z + v_0)$ in negative z direction. Ions are assumed to be cold satisfying $f_{i0} = \delta(v_x)\delta(v_y)\delta(v_z)$, where δ is the Dirac delta function. Furthermore, electron distribution function has been considered symmetric about $v_z = 0$ in order to neglect the current driven by the bump.[2] Thus, for studying bump-on-tail instability, we calculate the one dimensional kappa velocity distribution for electrons in the form

$$f_{e0}(v_z) = \int f_{e0}(v_x, v_y, v_z) dv_x dv_y = \frac{n_1}{n_e} \left(\pi\kappa\theta_1^2\right)^{-\frac{1}{2}} \frac{\Gamma(\kappa)}{\Gamma\left(\kappa-\frac{1}{2}\right)} \left[1 + \frac{v_z^2}{\kappa\theta_1^2}\right]^{-\kappa} + \frac{n_2}{n_e} \left(\pi\kappa\theta_2^2\right)^{-\frac{1}{2}} \frac{\Gamma(\kappa)}{\Gamma\left(\kappa-\frac{1}{2}\right)}$$

$$\times \frac{1}{2} \left[\left(1 + \frac{(v_z - v_0)^2}{\kappa\theta_2^2}\right)^{-\kappa} + \left(1 + \frac{(v_z + v_0)^2}{\kappa\theta_2^2}\right)^{-\kappa}\right]. \tag{8}$$

This distribution reduces to the one dimensional Maxwellian distribution as $\kappa \to \infty$.

Differentiating $f_{e0}(v_z)$ in (8) with respect to v_z, we get

$$\frac{\partial f_{e0}}{\partial v_z} = -\frac{2}{n_e \sqrt{\pi}\theta_1^3 \kappa^{3/2}} \frac{\Gamma(\kappa+1)}{\Gamma\left(\kappa-\frac{1}{2}\right)} \times \left[n_1 v_z \left(1 + \frac{v_z^2}{\kappa\theta_1^2}\right)^{-(\kappa+1)} + \frac{n_2}{2} \frac{\theta_1^3}{\theta_2^3} \left\{\left(1 + \frac{(v_z - v_0)^2}{\kappa\theta_2^2}\right)^{-(\kappa+1)} (v_z - v_0)\right.\right.$$

$$\left.\left. + \left(1 + \frac{(v_z + v_0)^2}{\kappa\theta_2^2}\right)^{-(\kappa+1)} (v_z + v_0)\right\}\right]. \tag{9}$$

Now assuming $n_1 \gg n_2$, $n_1 K_B T_1 \gg n_2 m_e v_0^2$, i.e., most of the particles and most of the energy are outside the bump, and substituting $\frac{\partial f_{e0}}{\partial v_z}$ from (9) into (4), we obtain

$$D_r = 1 - \frac{n_1}{n_e} \frac{\omega_{pe}^2}{\omega_r^2} - \frac{3}{2} \frac{n_1}{n_e} \frac{\omega_{pe}^2}{\omega_r^4} k_z^2 \left(\frac{\kappa}{\kappa - \frac{3}{2}}\right) \theta_1^2 = 1 - \frac{\omega_{p1}^2}{\omega_r^2} - 3k_z^2 \lambda_{D1}^2 \frac{\omega_{p1}^4}{\omega_r^4}, \tag{10}$$

where $\omega_{pe}^2 = \frac{4\pi n_e e^2}{m_e}$, $\omega_{p1}^2 = \frac{4\pi n_1 e^2}{m_e}$, $n_e = n_1 + n_2$, and $\lambda_{D1}^2 = \frac{k_B T_1}{4\pi n_1 e^2} = \left(\frac{\kappa}{2\kappa-3}\right) \frac{\theta_1^2}{\omega_{p1}^2}$.

Making $D_r = 0$, we obtain

$$\omega_r^2 = \omega_{p1}^2 (1 + 3k_z^2 \lambda_{D1}^2). \tag{11}$$

This is the same as square of the real frequency of Langmuir wave in a single humped Maxwellian plasma. Thus, the presence of the bump in the tail of the electron velocity distribution does not change the real frequency of the Langmuir wave. The real frequency of Langmuir wave also remains unchanged in the presence of suprathermal electrons.

Substitution of (9) in Eq. (6) with $v = v_z$ and $k = k_z$ gives

$$D_i = \frac{2\sqrt{\pi}\omega_{pe}^2}{k_z^2} \frac{1}{n_e \theta_1^3 \kappa^{3/2}} \frac{\Gamma(\kappa+1)}{\Gamma\left(\kappa-\frac{1}{2}\right)} \times \left[n_1 \frac{\omega_r}{k_z} \left(1 + \frac{\left(\frac{\omega_r}{k_z}\right)^2}{\kappa\theta_1^2}\right)^{-(\kappa+1)} + \frac{n_2}{2} \frac{\theta_1^3}{\theta_2^3} \left\{\left(1 + \frac{\left(\frac{\omega_r}{k_z} - v_0\right)^2}{\kappa\theta_2^2}\right)^{-(\kappa+1)} \left(\frac{\omega_r}{k_z} - v_0\right)\right.\right.$$

$$\left.\left. + \left(1 + \frac{\left(\frac{\omega_r}{k_z} + v_0\right)^2}{\kappa\theta_2^2}\right)^{-(\kappa+1)} \left(\frac{\omega_r}{k_z} + v_0\right)\right\}\right]. \tag{12}$$

Assumption of $k = k_z$ implies Langmuir wave is propagating in the z-direction. Now to calculate ω_i, we first differentiate equation (10) as follows:

$$\frac{\partial D_r}{\partial \omega_r} = \frac{2\omega_{p1}^2}{\omega_r^3} + 12 k_z^2 \lambda_{D1}^2 \frac{\omega_{p1}^4}{\omega_r^5}. \tag{13}$$

Substituting D_i and $\frac{\partial D_r}{\partial \omega_r}$ from (12) and (13) in (5), along with the approximations $n_1 \gg n_2$, $T_1 > T_2$, and $k_z \lambda_{D1} \ll 1$, we obtain the following growth rate:

$$\omega_i = \frac{\sqrt{\pi}}{(2\kappa-3)^{\frac{3}{2}}} \frac{\Gamma(\kappa+1)}{\Gamma\left(\kappa - \frac{1}{2}\right)} \frac{\omega_{p1}}{k_z^3 \lambda_{D1}^3} \times \left[\frac{n_2}{n_1} \left(\frac{T_1}{T_2}\right)^{\frac{3}{2}} \left(\frac{k_z v_0}{\omega_r} - 1\right) \left\{ 1 + \frac{T_1/T_2}{(2\kappa-3)k_z^2\lambda_{D1}^2}\left(1 - \frac{k_z v_0}{\omega_r}\right)^2 \right\}^{-(\kappa+1)} \right.$$
$$\left. - \left\{ 1 + \frac{1}{(2\kappa-3)k_z^2\lambda_{D1}^2} + \frac{3}{2\kappa-3} \right\}^{-(\kappa+1)} \right]. \tag{14}$$

This is the growth rate of the "bump-on-tail" instability of Langmuir waves in Lorentzian plasma. The first term in the bracket is the contribution from the positive tail of the distribution function where electrons resonate with Langmuir wave at phase velocity $\frac{\omega_r}{k_z}$. The second term corresponds to wave Landau damping. It needs to mention that contribution of the particles from the bump in the negative tail (Fig. 1) of the distribution function has been neglected as in that case this instability criterion depends on the position of the observer.

This growth rate ω_i is maximum when

$$\left| \frac{k_z v_0}{\omega_r} \right| = 1 + \sqrt{\frac{2\kappa-3}{2\kappa+1}} \sqrt{\frac{T_2}{T_1}} k_z \lambda_{D1}, \tag{15}$$

which gives $k_z \approx \frac{\omega_{p1}}{v_0}$ in the approximations $k_z \lambda_{D1} \ll 1$. Here, ω_r has been replaced by ω_{p1} as it is valid from (11) for $k_z \lambda_{D1} \ll 1$. Under this approximation, maximum growth rate becomes

$$\omega_{imax} = \frac{\sqrt{\pi}\omega_{p1}}{(2\kappa-3)^{\frac{3}{2}}k_z^3\lambda_{D1}^3} \frac{\Gamma(\kappa+1)}{\Gamma\left(\kappa-\frac{1}{2}\right)} \times \left[\frac{n_2 T_1}{n_1 T_2}\sqrt{\frac{2\kappa-3}{2\kappa+1}}\frac{m_e v_0^2}{K_B T_1}k_z^3\lambda_{D1}^3 \left\{\frac{2\kappa+2}{2\kappa+1}\right\}^{-(\kappa+1)} - \left\{1 + \frac{1}{(2\kappa-3)k_z^2\lambda_{D1}^2} + \frac{3}{2\kappa-3}\right\}^{-(\kappa+1)} \right], \tag{16}$$

which is a function of κ and other plasma parameters. Thus, unstable Langmuir waves propagate parallel to the particle velocity in the bump and attains maximum growth rate at $k_z \approx \frac{\omega_{p1}}{v_0}$.

IV. NUMERICAL ESTIMATION

The solar wind is a stream of charged particles released from the upper atmosphere of the Sun. The stream of particles varies in density, temperature, and speed over time and solar longitude. These particles can escape the sun's gravity because of their high kinetic energy due to high temperature of the solar corona. For these high energy particles, velocity distribution functions in solar wind are observed to be quasi Maxwellian up to the mean thermal velocities, while they have non Maxwellian suprathermal tails at higher velocities.[14] Such deviations from the Maxwellian distribution are well described by the kappa velocity distribution. Since the main objective of this paper is to study the bump-on-tail

instability in Lorentzian plasma with kappa distributed velocity of electrons, the analytical results obtained in Section III have been numerically estimated with solar wind data. In Section III, analytical expressions of the real frequency and the growth rate of the Langmuir wave have been found. Equation (11) shows that real frequency ω_r is independent of spectral index (κ), whereas Eqs. (14) and (16) show that growth rate and its maximum depend on κ values. In the limit of $\kappa \to \infty$, our results reduce to those in Ref. 2 where electron velocity distribution is Maxwellian. To estimate magnitude of the maximum growth rate of the instability with respect to different kappa indices, Fig. 3 has been plotted for $\omega_{imax}/\omega_{p1}$ versus κ for different n_1/n_2 ratios keeping T_1/T_2 fixed. Similarly, Fig. 4 has been plotted for the same $\omega_{imax}/\omega_{p1}$ versus κ for different T_1/T_2 ratios with n_1/n_2 fixed. The solar wind data $n_e = 8.7 \times 10^6 \text{m}^{-3}$, $T_1 = 2 \times 10^5 \text{K}$ have been considered to plot these graphs.[13–15] Temperature and number density (T_2, n_2) of the particles in
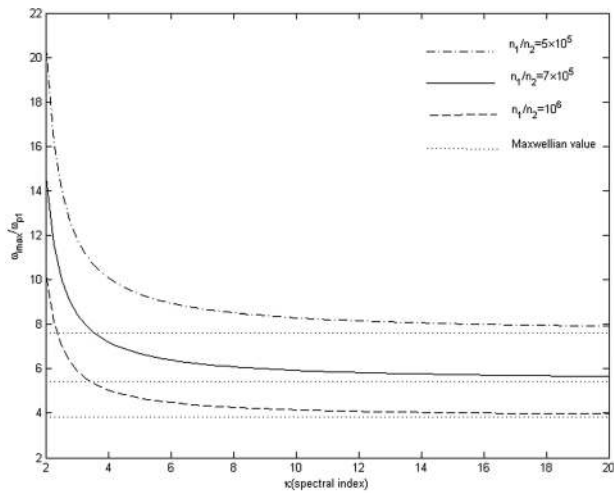
FIG. 3. Maximum growth rate of the instability as a function of spectral index (κ) at $n_1/n_2 = 5 \times 10^5, 7 \times 10^5, 10^6$ keeping T_1/T_2 fixed at 500.

the bump have been chosen according to the conditions $n_1 \gg n_2$, $n_1 K_B T_1 \gg n_2 m_e v_0^2$, and $k_z \lambda_{D1}$ has been considered of the order of 10^{-3}. Both Figs. 3 and 4 show that maximum growth rate is high at lower κ indices. As κ increases, the maximum growth rate rapidly falls and approaches to its value attained for the Maxwellian velocity distribution.[2]

Fig. 3 also indicates that growth rate of the instability is higher for smaller n_1/n_2 at fixed T_1/T_2, whereas Fig. 4 indicates higher growth rate for higher T_1/T_2 at fixed n_1/n_2. These indicate larger and thinner bump corresponds to stronger bump-on-tail instability. Although kappa distribution with $2 < \kappa < 6$ fits the observations and satellite data from the space plasmas,[6] the value of kappa has been considered
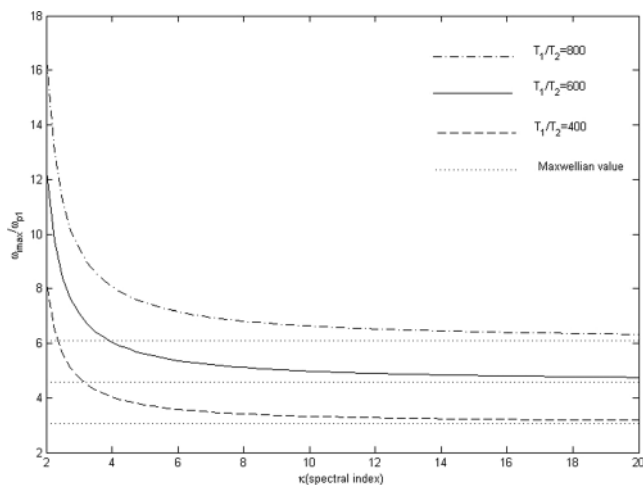
here 2 to 20 to verify that growth rate of the instability approaches to its Maxwellian value at higher κ.

V. CONCLUSION

In this paper, we have presented a complete description of bump-on-tail instability obtained from a systematic analysis of dispersion relation of Langmuir waves propagating in plasma modeled by a Lorentzian kappa velocity distribution with a spectral index κ(kappa). Analysis shows that maximum growth rate of the instability is high at lower kappa when sufficiently large number of suprathermal electrons are present. It decreases as κ increases and approaches to its Maxwellian value. This happens because the presence of larger number of suprathermal electrons at low κ transfer larger amount of energy to the Langmuir wave, which pronounces growth rate of the instability. As the number of suprathermal electrons decrease with increasing kappa, energy transfer from them to the wave will decrease, which consequently reduces the instability growth rate. Moreover, the magnitude of the maximum growth of the wave is high when the number density of electrons in the bump is high and temperature of the electrons in the bump is low. This implies that maximum growth rate of the instability increases with the increase in the number density and decrease in the temperature of suprathermal electrons streaming relative to the background plasma. All analytical results obtained in this paper agree with the results of Maxwellian plasma when kappa approaches to infinity. These are numerically confirmed in Figs. 3 and 4.

[1]T. M. J. Boyd and J. J. Sanderson, *Physics of Plasma* (Cambridge University Press, 2003), p. 269.
[2]N. A. Krall and A. W. Trivelpiece, *Principles of Plasma Physics* (McGraw-Hill, 1973), pp. 458–462.
[3]I. Zouganelis, J. Geophys. Res. **113**, A08111, doi:10.1029/2007JA012979 (2008).
[4]V. M. Vasyliunas, J. Geophys. Res. **73**, 2839, doi:10.1029/ JA073i009p02839 (1968).
[5]D. Summers and R. M. Thorne, Phys. Fluids. B **3**, 1835 (1991).
[6]V. Pierrard and M. Lazar, Sol. Phys. **267**, 153–174 (2010).
[7]D. Summers and R. M. Thorne, J. Geophys. Res: Space Phys. **97**(A11), 16827–16832 (1992).
[8]D. Summers and R. M. Thorne, J. Plasma Phys. **53**(03), 293–315 (1995).
[9]A. K. Tripathi and K. D. Misra, Earth, Moon, Planets **88**(3), 131–151 (2000).
[10]R. S. Pandey, R. P. Pandey, A. K. Srivastava, and K. Dubey, Ind. J. Radio Space Phys. **34**, 98–105 (2005).
[11]D.-H. Ki and Y.-D. Jung, Phys. Plasmas **18**, 014506 (2011).
[12]D. K. Kuri and N. Das, Phys. Plasmas **21**, 042016 (2014).
[13]J. A. Bittencourt, *Fundamentals of Plasma Physics* (Pergamon Press, 1986), p. 13.
[14]K. Issautier, N. M. Vernet, M. Moncuquet, and S. Hoang, J. Geophys. Res. **103**(a2), 1969–1979, doi:10.1029/97JA02661 (1998).
[15]K. Issautier, C. Perche, S. Hoang, C. Lacombe, M. Maksimovic, J. L. Bougeret, and C. Salem, Adv. Space Res. **35**, 2141–2146 (2005).

FIG. 4. Maximum growth rate of instability as a function of spectral index (κ) at $T_1/T_2 = 800, 600, 400$ keeping n_1/n_2 fixed at 10^6.